Experimental Neurology 320 (2019) 112983

Contents lists available at ScienceDirect

Experimental Neurology

journal homepage: www.elsevier.com/locate/yexnr

Research Paper

Melatonin alleviates asphyxial cardiac arrest-induced cerebellar Purkinje cell death by attenuation of oxidative stress

Jeong Hwi Cho[a,1], Hyun-Jin Tae[a,1], In-Shik Kim[a], Minah Song[b], Hyunjung Kim[b], Tae-Kyeong Lee[b], Young-Myeong Kim[c], Sungwoo Ryoo[d], Dae Won Kim[e], Choong-Hyun Lee[f], In Koo Hwang[g], Bing Chun Yan[h], Il Jun Kang[i], Moo-Ho Won[b,*], Jae-Chul Lee[b,*]

[a] Bio-Safety Research Institute, College of Veterinary Medicine, Chonbuk National University, Iksan, Jeollabuk-do 54596, Republic of Korea
[b] Department of Neurobiology, School of Medicine, Kangwon National University, Chuncheon 24341, Republic of Korea
[c] Department of Molecular and Cellular Biochemistry, School of Medicine, Kangwon National University, Chuncheon 24341, Republic of Korea
[d] Department of Biological Sciences, College of Natural Sciences, Kangwon National University, Chuncheon, Gangwon 24341, Republic of Korea
[e] Department of Biochemistry and Molecular Biology, Research Institute of Oral Sciences, College of Dentistry, Kangnung-Wonju National University, Gangneung 25457, Republic of Korea
[f] Department of Pharmacy, College of Pharmacy, Dankook University, Cheonan, Chungcheongnam 31116, Republic of Korea
[g] Department of Anatomy and Cell Biology, College of Veterinary Medicine, Research Institute for Veterinary Science, Seoul National University, Seoul 08826, Republic of Korea
[h] Institute of Integrative Traditional and Western Medicine, Medical College, Yangzhou University, Yangzhou, Jiangsu 225001, PR China
[i] Department of Food Science and Nutrition, Hallym University, Chuncheon, Gangwon 24252, Republic of Korea

ARTICLE INFO

Keywords:
Asphyxial cardiac arrest
Purkinje cells
Autophagy-like cell death
Melatonin
Melatonin receptor
Antioxidant enzymes

ABSTRACT

Although multiple reports using animal models have confirmed that melatonin appears to promote neuroprotective effects following ischemia/reperfusion-induced brain injury, the relationship between its protective effects and activation of autophagy in Purkinje cells following asphyxial cardiac arrest and cardiopulmonary resuscitation (CA/CPR) remains unclear. Rats used in this study were randomly assigned to 6 groups as follows; vehicle-treated sham operated group, vehicle-treated asphyxial CA/CPR operated group, melatonin-treated sham operated group, melatonin-treated asphyxial CA/CPR operated group, PDOT (a MT2 melatonin receptor antagonist) plus (+) melatonin-treated sham operated group and PDOT + melatonin-treated asphyxial CA/CPR operated group. Melatonin (20 mg/kg, i.p., 4 times before CA and 3 times after CA) treatment significantly improved survival rate and neurological deficit compared with the vehicle-treated asphyxial CA/CPR rats (survival rates ≥40% vs 10%), showing that melatonin treatment exhibited protective effect against asphyxial CA/CPR-induced Purkinje cell death. The protective effect of melatonin against CA/CPR-induced Purkinje cell death paralleled a remarkable attenuation of autophagy-like processes (Beclin-1, Atg7 and LC3), as well as a dramatic reduction in superoxide anion radical (O_2·-), intense enhancements of CuZn superoxide dismutase (SOD1) and MnSOD (SOD2) expressions. Furthermore, the protective effect was notably reversed by treatment with PDOT, which is a selective MT2 antagonist. In brief, melatonin conferred neuroprotection against asphyxial CA/CPR-induced Purkinje cell death via inhibiting autophagic activation by reducing expressions of O_2·- and increasing expressions of antioxidant enzymes, and suggests that MT2 is involved in neuroprotective effect of melatonin against Purkinje cell death caused by asphyxial CA/CPR.

1. Introduction

Experimental animal models of transient global cerebral ischemia (tgCI) resulting from cardiac arrest and cardiopulmonary resuscitation (CA/CPR) have been frequently used to examine injury mechanisms and neuroprotective therapies in vulnerable areas of the brain, such as the cerebral cortex, striatum and hippocampus (Fink et al., 2004). However, few studies have focused on the cerebellum following CA/CPR, despite data indicating that the cerebellum is vulnerable to tgCI (Paine et al., 2012; Welsh et al., 2002). In addition, Purkinje cells

* Corresponding authors.
E-mail addresses: mhwon@kangwon.ac.kr (M.-H. Won), anajclee@kangwon.ac.kr (J.-C. Lee).
[1] Both authors have contributed equally to this article.

https://doi.org/10.1016/j.expneurol.2019.112983
Received 3 December 2018; Received in revised form 7 June 2019; Accepted 22 June 2019
Available online 26 June 2019
0014-4886/

receive and integrate excitatory inputs from sensory, vestibular and motor areas to allow for temporally and spatially precise movement (Thach, 1998), and are also vulnerable to tgCI caused by CA/CPR; however, the time course of Purkinje cell death following CA/CPR is relatively controversial.

Melatonin (*N*-acetyl 5-methoxytryptamine) is primarily synthesized in the pineal gland and recognized as an interesting compound with physiological activity (Pandi-Perumal et al., 2006). Along with the relevant physiological roles, it has been reported that melatonin is capable of protecting the brain against ischemia/reperfusion injury by reducing oxidative damage (Chern et al., 2012; Ozacmak et al., 2009). In addition, effects of melatonin are mediated by two main pathways that include receptor-mediated and non-receptor mediated effects (Tan et al., 2007; Tomas-Zapico and Coto-Montes, 2005). The two major membrane-associated melatonin receptors, MT1 and MT2, are ubiquitously distributed in the central nervous system (CNS) as well as the peripheral organs (Drew et al., 2001). Furthermore, it has been demonstrated that, in the gerbil hippocampus, the activation of MT2 through melatonin treatment may be involved in neuroprotective action against tgCI (Lee et al., 2010). Although little is known about the influence of melatonin receptors on neuronal signaling during ischemic conditions, it is suggested that the melatonin receptor pathway may play roles in neuroprotective effects of melatonin against CA/CPR-induced injury.

Despite its label as catabolic process, autophagy is vital for cells to maintain the cellular homeostasis and the maintenance of cellular integrity (Yang and Klionsky, 2010). The activation of autophagy induces cell survival in ischemic cerebral injury, which could also promote cell death (Wei et al., 2012). To date, however, the contribution of autophagy to Purkinje cell death in the cerebellum following CA/CPR remains unclear. Therefore, in the present study, we attempted to identify the time course of Purkinje cell death following asphyxial CA/CPR in rats. In addition, we focused on the role of melatonin in Purkinje cell death and autophagy-like process caused by asphyxial CA/CPR, which is related to oxidative stress and antioxidant enzymes.

2. Materials and methods

2.1. Experimental animals and groups

Male Sprague-Dawley rats (10 weeks of age; body weight, 300–310 g) were used according to the experimental protocol, which was approved (approval no. KW-151127-1) by the Institutional Animal Care and Use Committee (IACUC) at Kangwon University.

Rats were divided into six groups (n = 14 at each point in time in each group: (1) vehicle-sham group, which was given vehicle treatment and sham operation (2) vehicle-CA group, which was given vehicle treatment and asphyxial CA/CPR operation, (3) melatonin-sham group, which was given melatonin treatment and sham operation, (4) melatonin-CA group, which was given melatonin treatment and asphyxial CA/CPR operation, (5) 4-phenyl-2-propionamidotetraline (PDOT) + melatonin-sham group, which was given PDOT + melatonin treatment and sham operation, (6) PDOT + melatonin-CA group, which was given PDOT + melatonin and asphyxial CA/CPR operation.

2.2. Melatonin and PDOT treatments

Melatonin (20 mg/kg, Sigma-Aldrich, St. Louis, MO, USA) and PDOT (10 mg/kg, Sigma-Aldrich), a selective MT2 antagonist, were dissolved with dimethyl sulfoxide (DMSO) and diluted with 0.9% saline to a final concentration of < 1% DMSO. Melatonin was intraperitoneally treated 7 times (once daily for 4 days before asphyxial CA/CPR operation, and at 30 min, 6 h and 1 day after asphyxial CA/CPR operation) based on previously published papers(Lee et al., 2010). PDOT was intraperitoneally administered at 10 min before every melatonin treatment. The dose of melatonin and PDOT was selected, respectively, on the basis of previous study (Chern et al., 2012).

2.3. Asphyxial CA/CPR operation

The experimental procedures were performed as previously described (Han et al., 2010) with minor modification. Briefly, the rats were anesthetized with a mixture of 2–3% isoflurane in 33% oxygen and 67% nitrous oxide and mechanically ventilated to maintain respiration using a rodent ventilator (Harvard Apparatus, Holliston, MA, USA). Body temperature was maintained at 37 ± 0.5 °C during the asphyxial CA surgery. Peripheral oxygen saturation (SpO_2) was monitored by an oxygen saturation probe of pulse oximetry (Nonin Medical Inc., Plymouth, MN, USA) that was attached to the left foot. Electrocardiogram (ECG) was monitored using electrocardiographic probes (GE healthcare, Milwaukee, WI, USA) which were placed to the limbs. Mean arterial pressure (MAP) was monitored via the left femoral artery using a blood pressure transducer (MP150, BIOPAC system, Goleta, CA, USA). After 5 min of stabilization period, vecuronium bromide (2 mg/kg, Reyon Pharmaceutical., Seoul, South Korea) were injected via the right femoral vein, and anesthesia was stopped. Mechanical ventilation was discontinued, and the endotracheal tube was disconnected from the ventilator. Mean arterial pressure (MAP) below 25 mmHg and isoelectric ECG were defined as asphyxial CA(Han et al., 2010). Usually, asphyxia CA was confirmed about 3–4 min after vecuronium bromide injection. After 5 min of asphyxial CA, CPR was initiated by administering a bolus injection of epinephrine (0.005 mg/kg, i.v. Dai Han Pharm, Seoul, South Korea) and sodium bicarbonate (1 meq/kg, i.v., Daewon Pham, Seoul, South Korea) followed by mechanical ventilation with 100% oxygen and mechanical chest compressions at a rate of 300/min until MAP reached 60 mmHg and electrocardiographic activity was observed (Liachenko et al., 1998). Once the animals were hemodynamically stable and spontaneously breathing (usually 1 h after return of spontaneous circulation (ROSC), the catheters were removed. Namely, at 2 h after resuscitation, the arterial and venous catheters were removed. The animals were then mechanically ventilated with room air and allowed to extubate themselves. Thereafter, animals were subcutaneously given 20 mL/kg/d isotonic saline with 5% dextrose until they could eat and drink without assistance.

2.4. Tissue processing for histology

The rats (n = 7 at each point in time) were anesthetized with pentobarbital sodium (30 mg/kg; JW Pharmaceutical, Seoul, South Korea) at designated times (sham, 12 h, 1 day and 2 days after asphyxial CA/CPR), and they were perfused transcardially with 0.1 M phosphate-buffered saline (PBS, pH 7.4) and fixed with 4% paraformaldehyde (in 0.1 M PB, pH 7.4). Their brains were removed and were serially cut into 30 μm frontal sections in a cryostat (Leica, Wetzlar, Germany).

2.5. Cresyl violet (CV) and Fluoro-jade B (F-J B) histofluorescence staining

To elucidate the neuronal damage induced by asphyxial CA/CPR, CV staining and F-J B histofluorescence were performed as previously described (Lee et al., 2017). Shortly, for CV staining, the sections were stained with 1.0% (*w/v*) CV acetate (Sigma–Aldrich) and dehydrated. They were then mounted with Canada balsam (Kanto chemical, Tokyo, Japan). For F-J B histofluorescence, the sections were immersed in a 0.0004% F-J B (Histochem, Jefferson, AR, USA) staining solution. After the stained sections were washed, they were examined using an epifluorescent microscope (Carl Zeiss, Göttingen, Germany) equipped with blue (450–490 nm) excitation light.

2.6. Immunohistochemistry

For immunohistochemical staining, the sections were carried out according to our previous method as previously described (Lee et al.,

2017). They were blocked with 15% normal goat serum (in 0.05 M PBS) and immunostained with primary antibodies, such as calbindin D-28 kDa (diluted 1:200, Chemicon International, Temecula, CA, USA), CuZn-superoxide dismutase (SOD1) (1:250, EMD Millipore, Billerica, MA, USA), Mn-SOD (SOD2) (1:200, EMD Millipore), catalase (CAT) (1:200, Abcam Incorporated, Cambridge, MA, UK), glutathione peroxidase (GPx) (1:200, Abcam Incorporated), MT1 (diluted 1:200; Santa Cruz Biotechnology, Santa Cruz, CA, USA), MT2 (diluted 1:200; Santa Cruz Biotechnology), Beclin-1 (diluted 1:200, Santa Cruz Biotechnology) overnight at 4 °C. The sections were next incubated with the biotinylated conjugated secondary antibodies and were visualized using Vectastain ABC Elite (Vector Laboratories Inc., Burlingame, CA, USA) with 0.5 mg/mL 3,3′-diaminobenzidine (Sigma-Aldrich).

2.7. Western blot analysis

To obtain exact data for alterations in levels of SOD1, SOD2, CAT, GPx, MT1, MT2, Beclin-1, Atg7 (Abcam Incorporated), LC3 (Santa Cruz Biotechnology) and β-actin (Abcam Incorporated) proteins in the cerebellar vermis after asphyxial CA/CPR, animals (n = 7 at each point in time) were killed at designated times (sham, 12 h, 1 day and 2 days) after asphyxial CA/CPR and used for western blot analysis as previously described (Lee et al., 2017).

2.8. Dihydroethidium fluorescence staining

To analyze oxidative stress, the brains (n = 7 at each point in time) were stained using dihydroethidium fluorescence staining at sham, 12 h, 1 day and 2 days after asphyxial CA/CPR. The oxidative fluorescent dyedihydroethidium (DHE; Sigma-Aldrich) was used to evaluate in situ production of superoxide anion radical (O_2·-). The histological detection of superoxide anion radical was performed as described previously (Lee et al., 2017).

2.9. Electron microscopic examination

Rats anesthetized with sodium pentobarbital (30 mg/kg; JW Pharmaceutical) were perfused transcardially with 0.1 M PBS and fixed with 2.5% glutaraldehyde (in 0.1 M PB). The cerebellar vermis tissues were cut into small pieces and more fixed in the same fixative for 3 h at 4 °C, and post-fixed with 1% osmium tetroxide (in 0.1 M PB) for 1.5 h at 4 °C. They were dehydrated in graded series of acetone dilution and embedded finally in Epon 812 epoxidic resin. Ultra-thin sections (40 nm) were made and stained with uranyl acetate and lead citrate. The stained samples were observed in Philips EM400 transmission electron microscope (TEM). Digital images from the samples were obtained using CCD camera (Gatan Orius; Gatan Inc., Pleasanton, CA, USA). During electron microscopic study on each Purkinje cell, 5 cytoplasmic fields in a grid were randomly captured. Measurement of autophagosomes was applied by using the ruler provided. Numbers of autophagic vacuoles were counted by two observers unaware of the experimental condition, and data were recorded. In estimating the size of the autophagic vacuoles, measurement along the largest diameter was taken and recorded.

2.10. Data analyses

Cell count was done according to our published method (Lee et al., 2017). In short, digital images were taken from 10 sections per animal by using a light microscope (AxioM1, Carl Zeiss) equipped with digital camera (Axiocam, Carl Zeiss) connected to a PC monitor. Calbindin D-28 kDa- and F-J B-positive cells in the PCL were counted in a 200 × 200 μm^2 area at the center of the PCL. Cell counts were obtained by averaging the counts from each animal. Quantification of neuronal counts in vulnerable regions of the brain is essential to understand the impact of neurological insults in animal models. Many researchers think that conventional qualitative protocols are superficial and less reliable for use in studies of neuroprotection evaluations. Stereology protocol is sensitive to medium-throughput counting of total neurons and consistent with comparable methods utilized for estimating neuronal injury. In this study, we focused on the Purkinje cell layer. It might be difficult to apply stereology to analyze cell numbers in the Purkinje cell layer. A commonly utilized technique to obtain quantitative information from histological sections is two-dimensional (2D) morphometry. With this technique, manual or automated analysis is performed on single or multiple tissue sections to obtain quantitative information, such as numbers of cells or other objects (linear measurements, or total area of positive staining after application of a cellular marker such as an immunohistochemical stain).

Ten sections per animal were selected for quantitative analyses of SOD1, SOD2, Beclin-1, MT1, MT2 immunoreactivity and superoxide anion fluorescence intensity in the PCL. With a previous method (Sugawara et al., 2002), the density of all immunoreactive structures and superoxide anion fluorescence intensity were evaluated on the basis of an optical density (OD), which was obtained after the transformation of the mean gray level using the formula: OD = log (256/mean gray level). After subtracting density of the background, ratio of the OD of the image file was calibrated using Adobe Photoshop 8.0 and analyzed as percent of relative optical density (ROD) compared with the sham-group, which was designated as 100% in NIH Image 1.59.

In addition, according to our previous method (Lee et al., 2017), we scanned results of western blotting, and carried out densitometric analyses for quantification of the bands using Scion Image software (Scion Corp., Frederick, MD). The expression rates of the target proteins were normalized through the corresponding expression rates of β-actin.

2.11. Statistical analysis

Sample size was at least seven rats per group with an alpha error of 0.05 and a power of > 80%, and the sample size was calculated with power calculator (UCLA Department of Statistics, http://www.stat.ubc.ca/~rollin/stats/ssize). All data are presented as mean ± S.E.M. A multiple-sample comparison was applied for testing differences between groups (ANOVA and the Tukey multiple range test as post hoc test using the criterion of the least significant differences). Statistical significance was considered at $p < 0.05$.

3. Results

3.1. Physiologic variables and survival rate after CA/CPR

Asphyxial CA/CPR was confirmed by isoeletric ECG, MAP and SpO_2 (Fig. 1A, B). The ECG, SpO_2 and MAP were changed as expected according to the experimental protocol.

Survival rate ($P < 0.05$) of the rats was determined by Kaplan-Meier analysis 2 days after asphyxial CA/CPR, as shown in Fig. 1C. In the vehicle-sham and melatonin-sham groups, the survival rate was 100%. However, survival rate in the vehicle-CA group was 33.3%, and survival rate in the melatonin-CA group was 46.7%.

3.2. Purkinje cell death caused by asphyxial CA/CPR

3.2.1. CV-positive (CV^+)

We examined the neuronal death of Purkinje cells in the cerebellar vermis after asphyxial CA/CPR using CV histochemistry (Fig. 2A). In the vehicle-sham group, CV^+ cells were found throughout the cerebellar vermis. In particular, CV^+ cells in the Purkinje cell layer, which are named Purkinje cells (cell body diameter > 30 μm), were relatively large and round in shape (Fig. 2A). In the vehicle-CA group, the morphology of CV^+ Purkinje cells was not changed 12 h after asphyxial CA/CPR (Fig. 2A). However, CV^+ Purkinje cells were significantly damaged 1 day after asphyxial CA/CPR. The damaged CV^+ Purkinje cells were

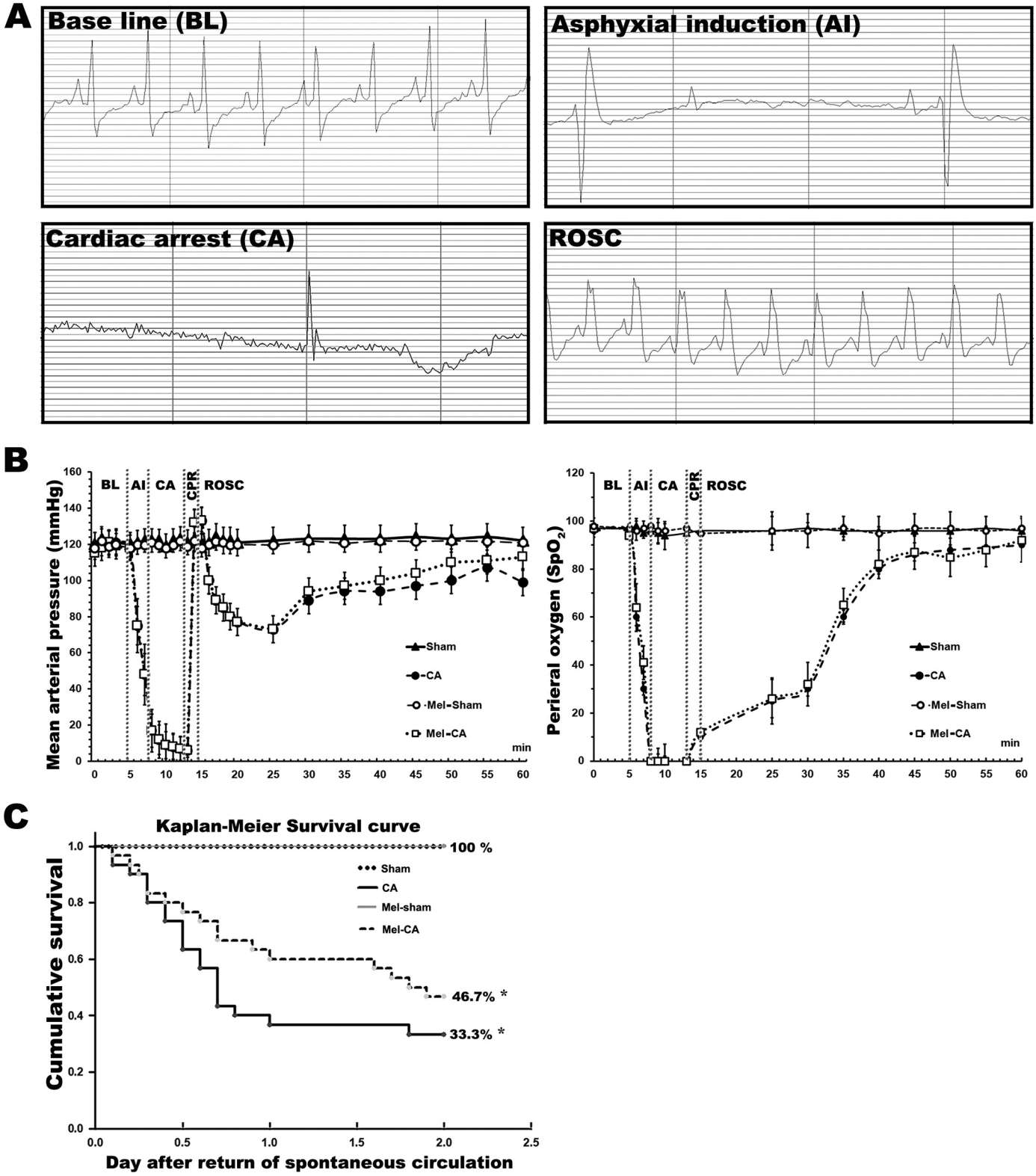

Fig. 1. Physiologic variables and survival rate after asphyxial CA/CPR.
(A) Electrocardiogram (ECG) from a representative animal at base line (BL), asphyxia induction (AI), CA and return of spontaneous circulation (ROSC) in the vehicle-CA group. Pulseless electrical activity is shown during CA, although it is often visible during CA. (B) Mean arterial pressure (MAP) and SpO_2 levels during CA, CPR and ROSC. (C) Cumulative survival rate (log-rank test, $p < 0.05$) using Kaplan-Meier analyses in each group for 2 days after asphyxial CA/CPR.

darkened and shrunken (Fig. 2A). Two days after asphyxial CA/CPR, CV^+ Purkinje cells were hardly detected (Fig. 2A).

3.2.2. Calbindin D-28 kDa$^+$ and F-J B$^+$ cells

To examine Purkinje cell death after asphyxial CA/CPR, sections of the cerebellar vermis were labeled with anti-calbindin D-28 kDa (a general marker for Purkinje cells) immunohistochemistry and F-J B (a

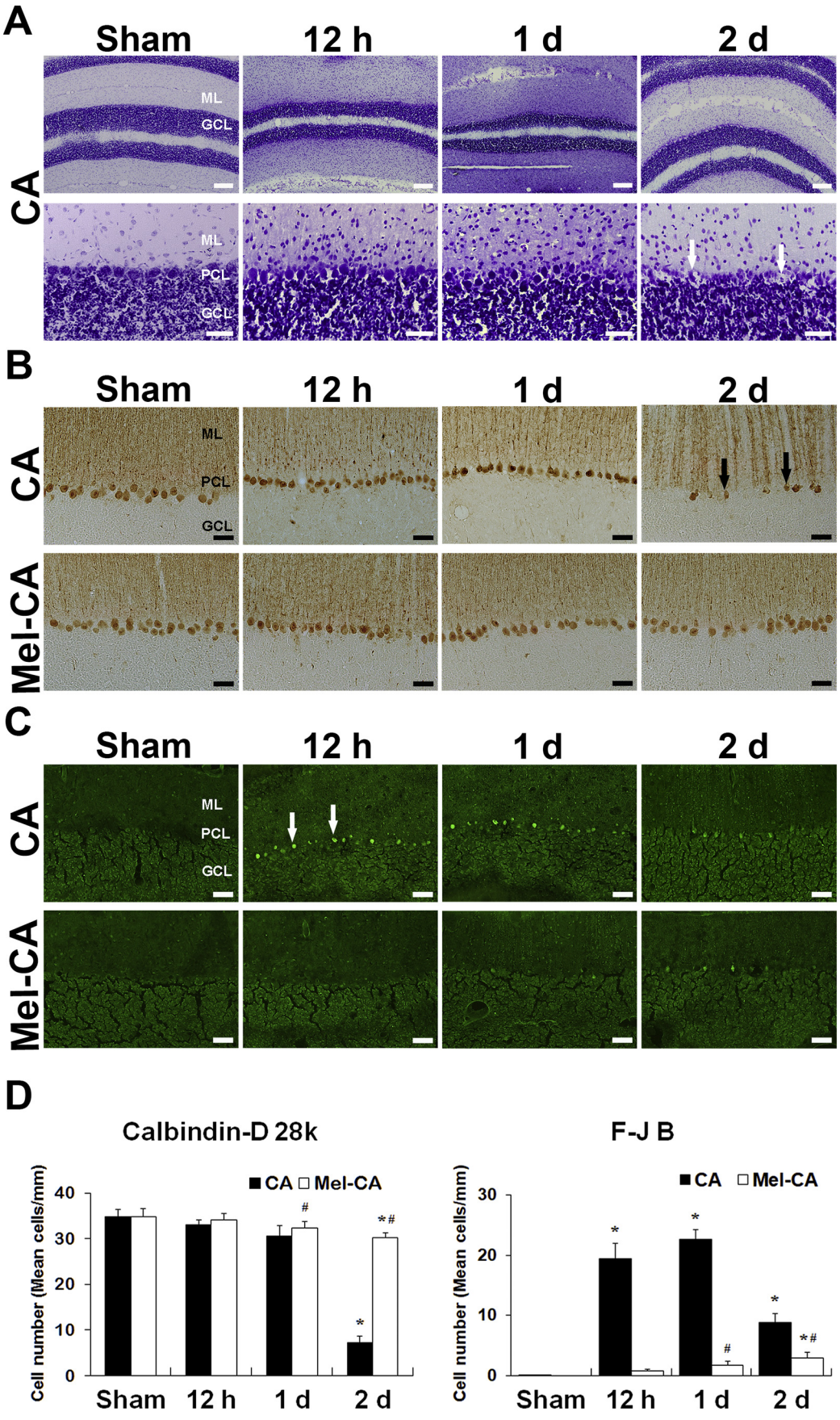

Fig. 2. Protection against Purkinje cell death caused by asphyxial CA/CPR by melatonin.
(A) CV staining for Purkinje cell degeneration in the cerebellum of the vehicle-CA group at sham, 12 h, 1 day and 2 days after asphyxial CA/CPR. GCL, granular cell layer; MCL, molecular cell layer; Purkinje cell layer; PCL. Scale bar = 800 and 50 μm. (B and C) Calbindin D-28 kDa immunohistochemistry (B) and F-J B histofluorescence staining (C) in the cerebellum of the vehicle- and melatonin-CA groups at sham, 12 h, 1 day and 2 days after asphyxial CA/CPR. Scale bar = 50 μm. (D) Quantitative graph of numbers of calbindin D-28 kDa$^+$ and F-J B$^+$ cells in the PCL. The bars are reported as means ± SEM (n = 7, $^*p < 0.05$ vs. vehicle-sham group; $^\#p < 0.05$ vs. vehicle-CA group).

fluorescent marker for neuronal degeneration) histofluorescence staining (Fig. 2B–D). In the vehicle-sham and vehicle-CA groups, Purkinje cells were well stained with calbindin D-28 kDa (Fig. 2B, D), and no F-J B^+ cells were found (Fig. 2C, D). We did not find significant change in numbers of calbindin D-28 kDa^+ Purkinje cells at 12 h post-CA/CPR (Fig. 2B, D); however, at this point in time, many F-J B^+ cells were observed (Fig. 2C, D). At 1 day after asphyxial CA/CPR, the number of calbindin D-28 kDa^+ Purkinje cells was slightly deceased (Fig. 2B, D), and the number of F-J B^+ cells was significantly increased (Fig. 2C, D). Two days after asphyxial CA/CPR, a significant loss of calbindin D-28 kDa^+ Purkinje cells (7.9% of the vehicle-sham group) was shown, and the number of F-J B^+ cells was decreased compared to that at 1 day post-CA/CPR (Fig. 2B–D).

3.3. Protection of asphyxial CA/CPR-induced Purkinje cell death by melatonin

3.3.1. Calbindin D-28 kDa^+ and F-J B^+ cells

In the melatonin-sham group, the distribution of calbindin D-28 kDa^+ Purkinje cells was similar to that in the vehicle-sham group (Fig. 2B, D), and no F-J B^+ cells were found (Fig. 2C, D). In the melatonin-CA group, abundant calbindin D-28 kDa^+ Purkinje cells were found, and F-J B^+ cells were rarely shown. Namely, Purkinje cells were well protected by melatonin: calbindin D-28 kDa^+ Purkinje cells were 86.8% of the vehicle-sham group, and F-J B^+ cells were 7.9% of the vehicle-CA group at 2 days after asphyxial CA/CPR (Fig. 2B–D).

3.4. Abolishment of melatonin-mediated neuroprotection by MT2 receptor inhibition

3.4.1. Levels and immunoreactivities of melatonin receptors

An important component of melatonin action resides in the presence of its MT1 and MT2 receptors. In western blotting, relative expressions of melatonin receptors were evaluated between the vehicle-sham and melatonin-sham groups (Fig. 3A). Levels of MT2 in both groups were higher than MT1 levels. In immunohistochemistry, MT1 immunoreactivity was very weak in all layers of the vehicle-sham group (Fig. 3B). However, strong MT2 immunoreactivity was shown in Purkinje cells of the vehicle-sham group (Fig. 3B).

3.4.2. Calbindin D-28 kDa^+ and F-J B^+ cells

In the PDOT-sham and the PDOT + melatonin-sham groups, the distribution of calbindin D-28 kDa^+ Purkinje cells was similar to that in the vehicle-sham group (Fig. 3C), and no F-J B^+ Purkinje cells were found (Fig. 3D). In addition, the PDOT-CA and the PDOT + melatonin-CA groups showed that change patterns of calbindin D-28 kDa^+ and F-J B^+ Purkinje cells after asphyxial CA/CPR were similar to those in the vehicle-CA group (Fig. 3C, D).

3.5. Attenuation of asphyxial CA/CPR-induced activation of autophagy by melatonin via MT2 receptor

3.5.1. Beclin-1, Atg7 and LC3 protein levels

The western analysis revealed that expressions of Beclin-1, Atg7 and ratio of LC3-II/LC3-I protein were significantly increased at 12 h after asphyxial CA/CPR compared to the vehicle-sham groups and peaked 1 day after asphyxial CA/CPR. However, these proteins levels were significantly decreased 2 days after asphyxial CA/CPR (Fig. 4A). In the melatonin-sham group, expressions of Beclin-1, Atg7 and ratio of LC3-II/LC3-I protein were similar to those in the vehicle-sham group (Fig. 4A). In the melatonin-CA groups, expressions of Beclin-1, Atg7 and ratio of LC3-II/LC3-I protein were not significantly altered (Fig. 4A). In addition, in the PDOT + melatonin-sham group, expressions of Beclin-1, Atg7 and ratio of LC3-II/LC3-I protein were similar to those in the vehicle-sham group (Fig. 4A). PDOT treatment into the melatonin-CA group showed that expressions of Beclin-1, Atg7 and ratio of LC3-II/

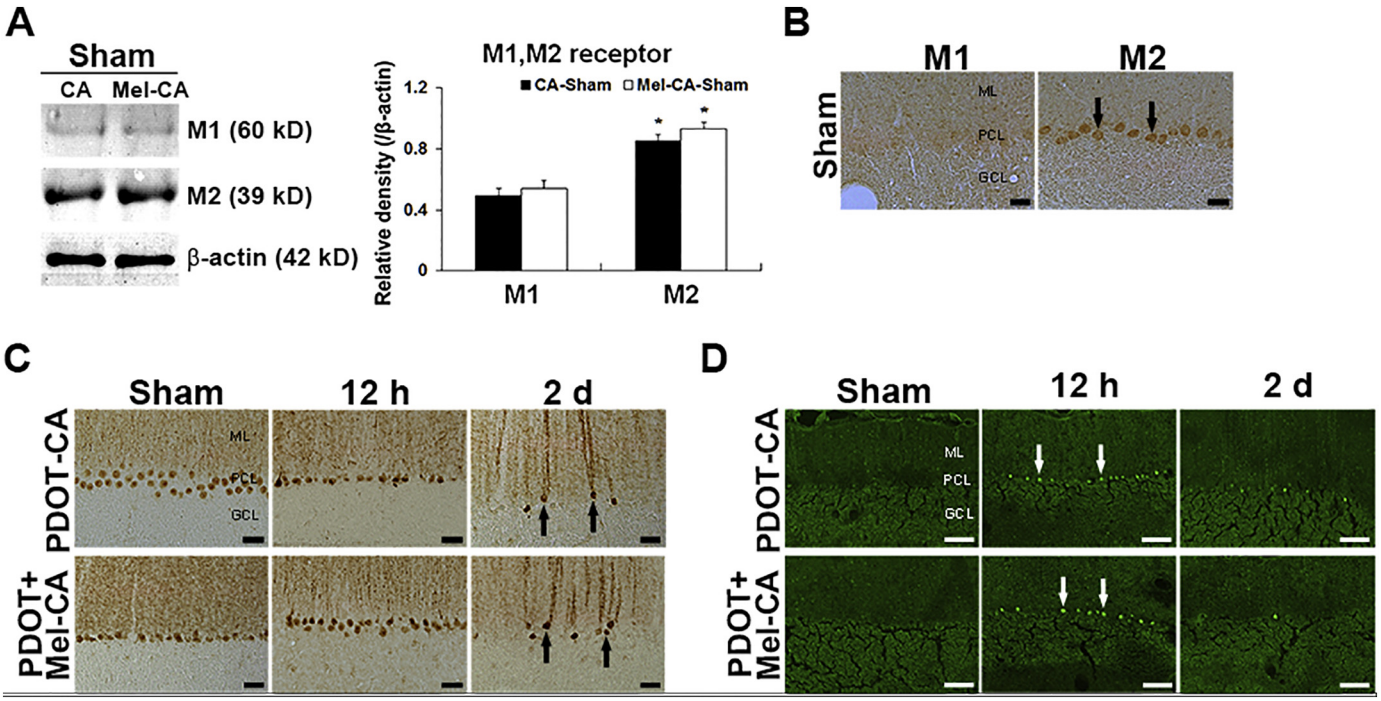

Fig. 3. Attenuation of Purkinje cell death caused by asphyxial CA/CPR by melatonin via MT2 receptor.
(A) Western blotting of melatonin receptors levels from the cerebellar vermis of the vehicle-sham and melatonin-sham groups. Protein expression is normalized to β-actin. The bars are reported as means ± SEM (n = 7, *p < 0.05 vs. MT1). (B) Immunohistochemistry for MT1 and MT2 in the cerebellar vermis of the vehicle-sham and melatonin-sham groups. GCL, granular cell layer; MCL, molecular cell layer; PCL, Purkinje cell layer. Scale bar = 50 μm. (C and D) Calbindin D-28 kDa immunohistochemistry (C) and F-J B histofluorescence staining (D) in the cerebellum of the PDOT- and PDOT + melatonin-CA groups at sham, 12 h and 2 days after asphyxial CA/CPR. Scale bar = 50 μm.

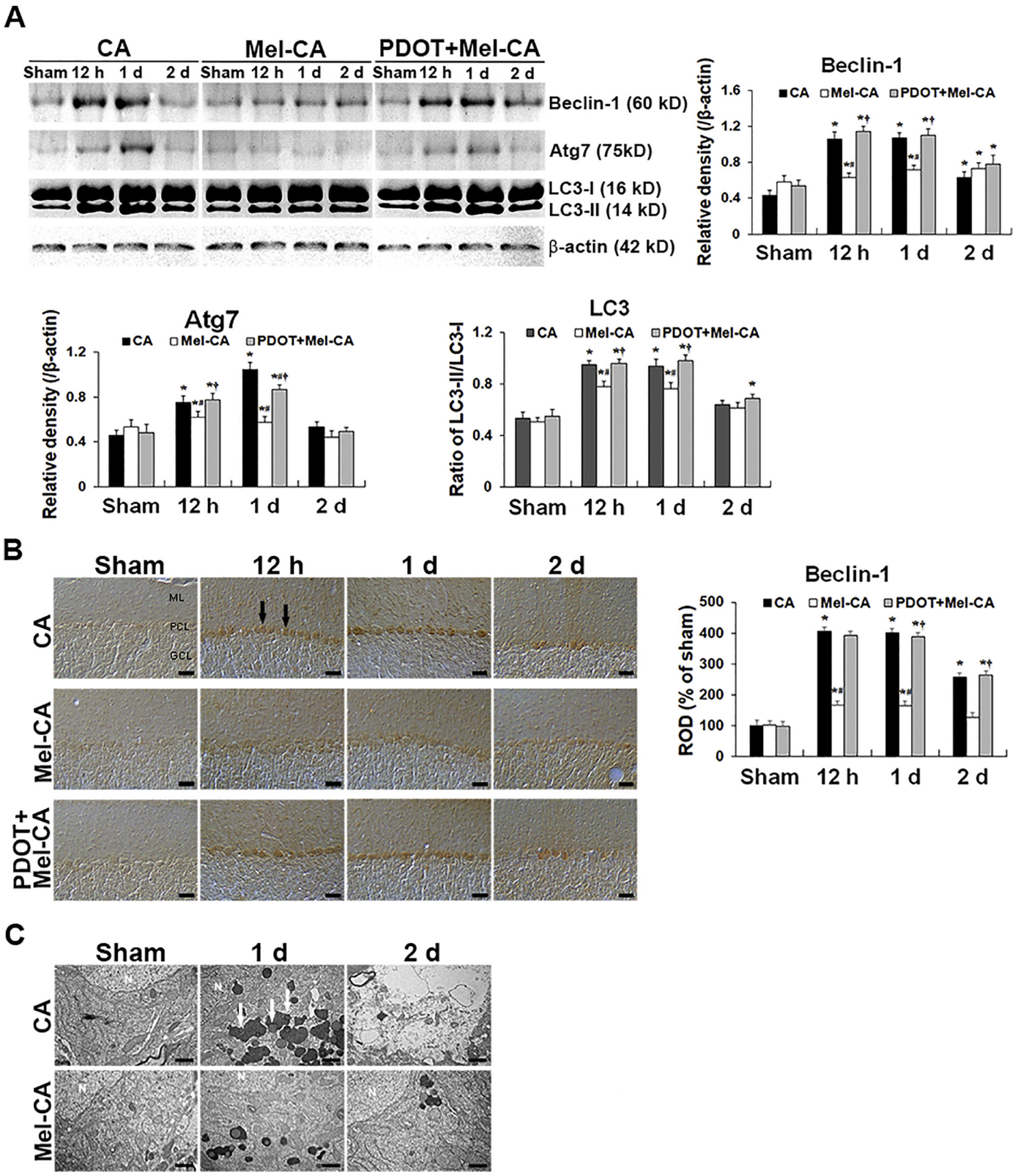

Fig. 4. Effect of melatonin against autophagy caused by asphyxial CA/CPR via MT2 receptor.
(A) Western blot analyses of Beclin-1, Atg7, and ratio of LC3-II/LC3-I protein levels in the vehicle-CA and melatonin-CA and melatonin + PDOT-CA groups after asphyxial CA/CPR. Protein expressions are normalized to β-actin. The bars are reported as means ± SEM (n = 7, *$p < 0.05$ vs. vehicle-sham group; $^{\#}p < 0.05$ vs vehicle-CA group; $^{\dagger}p < 0.05$ vs melatonin-CA group). (B) Immunohistochemistry of Beclin-1 in the vehicle-CA and melatonin-CA and melatonin/PDOT-CA groups at sham, 12 h, 1 day and 2 days after CA/CPR. GCL, granular cell layer; MCL, molecular layer; PCL, Purkinje cell layer. Scale bar = 50 μm. A ratio of the ROD was calibrated as % compared to the vehicle-sham group designated as 100%. The bars are reported as means ± SEM (n = 7, *$p < 0.05$ vs. vehicle-sham group; $^{\#}p < 0.05$ vs. vehicle-CA group; $^{\dagger}p < 0.05$ vs. melatonin-CA group). (C) Ultrastructural changes in Purkinje cells in the vehicle-CA and melatonin-CA groups at sham, 1 day and 2 days after asphyxial CA/CPR. N, nucleus. Scale bar = 1 μm.

LC3-I protein were significantly increased compared to the melatonin-CA group (Fig. 4A).

3.5.2. Beclin-1 immunoreactivity

Beclin-1 immunoreactivity in the vehicle-sham group was weakly observed in Purkinje cells (Fig. 4B). In the vehicle-CA group, Beclin-1 immunoreactivity was intensely increased in Purkinje cells at 12 h (Fig. 4B) and peaked 1 day after asphyxial CA/CPR (Fig. 4B). Thereafter, Beclin-1 immunoreactivity was markedly decreased 2 days after asphyxial CA/CPR (Fig. 4B). In the melatonin-sham group, Beclin-1 immunoreactivity in Purkinje cells was similar to that in the vehicle-sham group (Fig. 4B). In the melatonin-CA groups, Beclin-1 immunoreactivity in Purkinje cells was slightly increased 12 h and 1 day after asphyxial CA/CPR and not significantly altered 2 days after asphyxial CA/CPR compared to the vehicle-CA group (Fig. 4B). In the PDOT + melatonin-sham group, Beclin-1 immunoreactivity in Purkinje cells was similar to that in the vehicle-sham group (Fig. 4B). However, in the PDOT + melatonin-CA groups, its change pattern was similar to that in the vehicle-CA group (Fig. 4B).

3.5.3. Electron microscopic examination

In the vehicle-sham group, Purkinje cells showed typical morphological features of normal cell (Fig. 4C). They had few or no autophagic vesicles in their cytoplasm (Fig. 4C). However, in the vehicle-CA groups, autophagic vesicles were significantly accumulated in the perikaryon of Purkinje cell at 1 day after asphyxial CA/CPR, and the size and complexity of the autophagic vesicles was significantly higher than that in the vehicle-sham group (Fig. 4C). Two days after asphyxial CA/CPR, most Purkinje cells exhibited many vacuolated appearances in their cytoplasm (Fig. 4C). In addition, their cytoplasm was very pale and had scanty or damaged organelles (Fig. 4C). Furthermore, nuclear membranes were disrupted (Fig. 4C). In the melatonin-sham group, the ultrastructure of cerebellar Purkinje cells was similar to that in the vehicle-sham group (Fig. 4C). In the melatonin-CA group, cytoplasm and organelles of Purkinje cells were hardly damaged at 1 and 2 days after asphyxial CA/CPR (Fig. 4C). In addition, numbers of autophagic vesicles in Purkinje cells were significantly decreased compared to the vehicle-CA group (Fig. 4C).

3.6. Attenuation of asphyxial CA/CPR-induced oxidative stress by melatonin via MT2 receptor

3.6.1. DHE fluorescence

In the vehicle-sham group, $O_2^{\cdot-}$ level by DHE fluorescence was very weakly detected in Purkinje cells (Fig. 5A). In the vehicle-CA group, $O_2^{\cdot-}$ production was significantly increased in Purkinje cells 12 h (Fig. 5A) and peaked 1 day after asphyxial CA/CPR. Thereafter, $O_2^{\cdot-}$ production was significantly decreased 2 days after asphyxial CA/CPR (Fig. 5A). In the melatonin-sham group, $O_2^{\cdot-}$ level in Purkinje cells was similar to that in the vehicle-sham group (Fig. 5A). In the melatonin-CA group, $O_2^{\cdot-}$ level was significantly low compared with that of the corresponding vehicle-CA group (Fig. 5A). In the PDOT-sham group, $O_2^{\cdot-}$ level in Purkinje cells was similar to that in the vehicle-sham (Fig. 5A). In the PDOT + melatonin-CA group, $O_2^{\cdot-}$ production was intensely increased in Purkinje cells 12 h and 1 day after asphyxial CA/CPR, and, 2 days after asphyxial CA/CPR, $O_2^{\cdot-}$ level in Purkinje cells was significantly decreased (Fig. 5A).

3.6.2. Levels of antioxidant enzymes

Levels of SOD1 and SOD2 protein in the vehicle-CA group were gradually and significantly decreased from 12 h and peaked 2 days after asphyxial CA/CPR compared to those in the vehicle-sham group (Fig. 5B). In the melatonin-CA group, SOD1 and SOD2 protein levels were not significantly altered at any times after asphyxial CA/CPR (Fig. 5B). Change patterns of SOD1 and SOD2 protein levels in the PDOT + melatonin-CA group were similar to those in the vehicle-CA groups (Fig. 5B). However, CAT protein levels in all groups were not significantly changed after asphyxial CA/CPR (Fig. 5B). Levels of GPx-1 protein in the vehicle-CA group were gradually and significantly decreased from 1 day and peaked 2 days after asphyxial CA/CPR compared to the vehicle-sham group. In the melatonin-CA and PDOT + -melatonin-CA groups, the change pattern of GPx-1 protein levels was similar to that in the vehicle-CA group (Fig. 5B).

3.6.3. Immunoreactivities of antioxidant enzymes

Immunoreactivities of SOD1 and SOD2 were detected in Purkinje cells in the vehicle-sham group (Fig. 6A, B). In the vehicle-CA groups, SOD1 and SOD2 immunoreactivities in Purkinje cells were gradually and significantly decreased with time from 12 h after asphyxial CA/CPR and hardly observed 2 days after asphyxial CA/CPR (Fig. 6A, B). In the melatonin-sham group, SOD1 and SOD2 immunoreactivities in Purkinje cells were similar to those in the vehicle-sham group (Fig. 6A, B). In the melatonin-CA group, SOD1 and SOD2 immunoreactivities were not changed (Fig. 6A, B). In the PDOT/melatonin-sham group, SOD1 and SOD2 immunoreactivities were similar to those in the vehicle-sham group (Fig. 6A, B). In the PDOT + melatonin-CA group, their change patterns were similar to those in the vehicle-CA group (Fig. 6A, B).

4. Discussion

In the central nervous system, specific brain areas are selectively damaged, even after a brief ischemic episode, and this topographical heterogeneity is described as “selective vulnerability of the brain”. The hippocampus is well known for being one of the most vulnerable regions of the brain to ischemia. Specifically, neuronal death in the hippocampal CA1 region occurs with a delayed onset of 3–4 days after ischemia-reperfusion, described as “delayed neuronal death” (Kirino, 1982). Purkinje cells are also one of the most sensitive cells to cerebral ischemia (Paine et al., 2012; Welsh et al., 2002), relatively little is known about when Purkinje cells are damaged by ischemia. In addition, the time course of Purkinje cell death induced by ischemia-reperfusion is inconsistent according to models of ischemia-reperfusion (i.e., tgCI and CA/CPR), duration of transient ischemia, and/or animal species used. First, damage by asphyxial CA/CPR might be different from damage by tgCI. Compared with tgCI induced by traditional occlusion of main arteries to the brain (common carotid and vertebral arteries), asphyxial CA/CPR completely stops blood flow to entire organisms, producing a concurrent trauma to the hindbrain. In this study, we utilized a rat model of asphyxial CA/CPR, which developed whole body ischemia-reperfusion injury (Paine et al., 2012). Although this technique relies on chemical paralysis and cessation of ventilation to induce circulatory arrest, this technique is reliable and reproducible. Second, the degeneration of Purkinje cells showed a slightly delayed time course of 4 days after CA/CPR in humans(Horn and Schlote, 1992). Welsh et al. (2002) reporetd that the death of Purkinje cells were killed up to 47% by 10.5 min of global brain ischemia in rats. Brasko et al. demonstrated that over 60% of Purkinje cells were lost in 7 days following a 10 min of CA in rats (Brasko et al., 1995). Recently, Quillinan et al. (2015) reported that about 24% of Purkinje cells were killed between 1 and 7 days after 8 min CA in mice. In this study, we found that Purkinje cells were quickly killed following a 5 min of asphyxial CA and about 92.1% of Purkinje cells were lost at 2 days after the CA. Our results indicate that Purkinje cell death in a rat model of asphyxial CA/CPR occurs with a more rapid time course than that in other animal models.

Previous works have demonstrated that melatonin exhibits neuroprotective effects against ischemic brain injury (Cervantes et al., 2008; Lee et al., 2010). Moreover, our previous study showed that melatonin provided significant protection against hippocampal neuronal cell damage in a rat model of chronic cerebral hypoperfusion (Lee et al., 2016). To date, there are hardly any studies reporting effects of melatonin against Purkinje cell death caused by asphyxial CA/CPR. Here, we observed that the melatonin-treated rats exhibited a significant

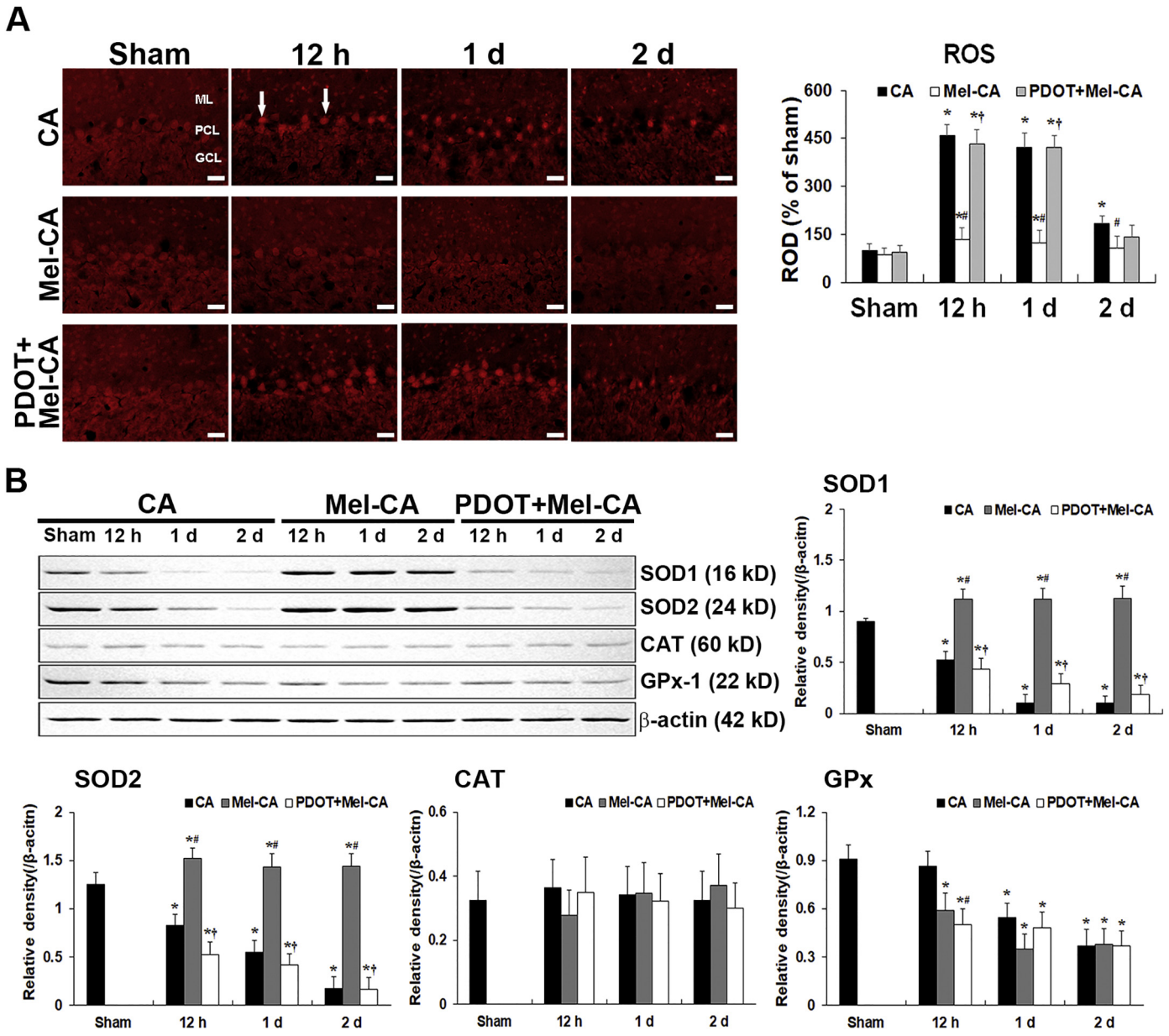

Fig. 5. Effect of melatonin on asphyxial CA/CPR-induced oxidative stress via MT2.
(A) Oxidative fluorescent staining for DHE in the cerebellar vermis of the vehicle-CA, melatonin-CA and PDOT + melatonin-CA groups at sham, 12 h, 1 day and 2 days after asphyxial CA/CPR. GCL, granular cell layer; MCL, molecular cell layer; PCL, Purkinje cell layer. Scale bar = 50 μm. A ratio of the ROD was calibrated as %, with the vehicle-sham group designated as 100%. The bars are reported as means ± SEM (n = 7, *$p < 0.05$ vs. vehicle-sham group; $^{\#}p < 0.05$ vs. vehicle-CA group; $^{\dagger}p < 0.05$ vs. melatonin-CA group). (B) Western analyses of SOD1, SOD2, CAT and GPx proteins in the vehicle-CA, melatonin-CA and PDOT + melatonin-CA groups. Protein expressions are normalized to β-actin. The bars are reported as means ± SEM (n = 7, *$p < 0.05$ vs. vehicle-sham group; $^{\#}p < 0.05$ vs. vehicle-CA group; $^{\dagger}p < 0.05$ vs. melatonin-CA group).

decrease in Purkinje cell death following asphyxial CA/CPR. Among actions of melatonin, a previous study has shown that melatonin elicits protective effects against ischemia/reperfusion injury by attenuating free radical production through MT2 (Yu et al., 2014). Chern et al. (2012) have also reported that melatonin ameliorates neural function in mice with ischemic-stroke by promoting endogenous neurogenesis and preservation of BBB integrity through MT2. In addition, it has been reported that the activation of MT2 in the hippocampal CA1 region following melatonin treatment is associated with neuroprotective effects against tgCI in gerbils (Lee et al., 2010). In this study, the expression of MT2 was observed in Purkinje cells, and protective effect of melatonin was reversed by treatment with PDOT, which is a selective MT2 antagonist, indicating that the protective effect of melatonin might be due to the action of MT2 receptor.

In ischemic cerebral injury, the activation of autophagy has been considered a double-edged sword with pro-survival or pro-death potential against ischemic cerebral injury (Wei et al., 2012). However, excessive activation of autophagy could induce cell death after reperfusion due to degeneration of too many organelles and proteins (Koike et al., 2008; Wen et al., 2008). Thus, the role of autophagy in neuronal death/survival remains to be defined under ischemic conditions of asphyxial CA/CPR. In addition, no studies have investigated the role of melatonin in the regulation of autophagy against Purkinje cell death caused by asphyxial CA/CPR. Therefore, to determine whether asphyxial CA/CPR activates excessive autophagy-like process in Purkinje cells, we performed both biochemical and morphological

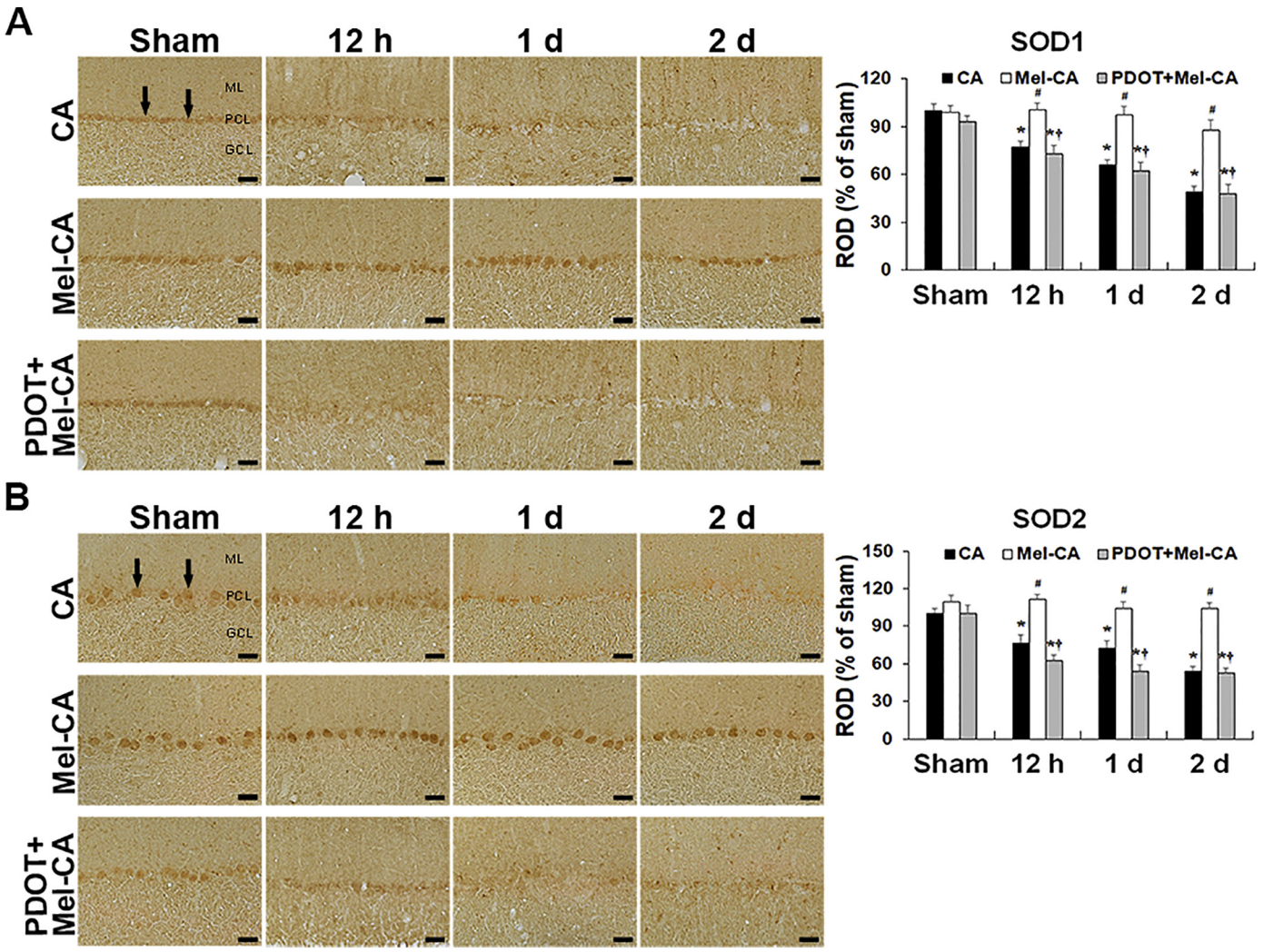

Fig. 6. Effect of melatonin on immunoreactivities of antioxidant enzymes after asphyxial CA/CPR.
(A and B) Immunohistochemistry for SOD1 (A) and SOD2 (B) in the vehicle-CA, melatonin-CA and PDOT + melatonin-CA groups at sham, 12 h, 1 day and 2 days after asphyxial CA/CPR. GCL, granular cell layer; MCL, molecular cell layer; PCL, Purkinje cell layer. Scale bar = 50 μm. A ratio of the ROD was calibrated as % compared with the vehicle-sham group designated as 100%. The bars indicate the means ± SEM (n = 7, *$p < 0.05$ vs. vehicle-sham group; $^{\#}p < 0.05$ vs. vehicle-CA group; $^{\dagger}p < 0.05$ vs. melatonin-CA group).

assessments, combined with various autophagy-related markers (Beclin-1, Atg7 and LC3). Beclin-1, which is the homolog of yeast autophagy gene 6, is a component of phosphatidylinositol type III 3-kinase complex that requires autophagosome formation (Yu et al., 2014). Based on its role, enhanced Beclin-1 expression has been used as a marker to estimate dynamic changes in the activation of autophagy (Kihara et al., 2001; Qu et al., 2003). Some reports have shown that cerebral ischemia induces the upregulation of Beclin-1 expression and autophagy-like cell death (Liu et al., 2012; Rami et al., 2008). In addition, Autophagy proceeds via a complex interplay of autophagy-related genes (Atg), with Atg7 representing a central component (Mizushima et al., 1998). A major player in the regulation of autophagy Atg7 is the ubiquitin E1-like enzyme that controls the critical step of converting Atg8/LC3-I to LC3-II through covalent attachment of phosphatidylethanolamine (Ichimura et al., 2000). In the current study, we showed that upregulations of Beclin-1 and Atg7 were detected in the cerebellum from 12 h to 1 day after asphyxial CA/CPR. Also, a dramatic elevation of Beclin-1 immunoreactivity was observed in Purkinje cells following asphyxial CA/CPR, especially in its immunohistochemical study. Rami et al. (2008) showed a dramatic upregulation of LC3-II in the rat brain following cerebral ischemia and suggested that the activation of autophagy was induced by brain ischemic injury. In the present study, the expression of LC3-I in the cerebellum during the period of asphyxial CA/CPR injury showed no significant upregulation. Moderate LC3-II expression bands were detected in the sham cerebellum, and the expression of LC3-II increased at 12 h and peaked at 1 day after asphyxial CA/CPR. Interestingly, the time courses and levels of Beclin-1 and Atg7 expressions correlated well with the increase of LC3-II to LC3-I ratios. Furthermore, the conversion from LC3-I to LC3-II might be closely correlated with autophagosome formation (Liu et al., 2010). The most traditional method to monitor autophagy utilizes electron microscopy. As results, autophagosomes enclosing cellular cargo can be easily distinguished from other cellular membranous compartments by using electron microscopy. However, in comparison to autophagosomes, distinction between autolysosomes and other membranous compartments is very difficult because autolysosomes have a single limiting membrane and contain cytoplasmic materials at various stages of degradation. It is important to note that vacuoles containing no or little inside materials are not autophagic structures (phagophores, autophagosomes and autolysosomes) (Eskelinen, 2005; Tsvetkov et al., 2010). Although electron microscopy has emerged as a useful tool to study autophagy, this method requires specialized skills. In this study, we counted autophagic vesicles in the cytoplasm of Purkinje cell for autophagic organelles, because autophagosome fuses with

lysosome possessing hydrolases to generate autophagolysosome. Under a TEM, Purkinje cells at 1 day after asphyxial CA/CPR were observed in increased structures of autophagic and lysosomal bodies with cytoplasmic material and enhanced electron density in this study. This finding indicates that autophagy is significantly increased in Purkinje cells that are degenerating as a product of asphyxial CA/CPR. Therefore, we suggest that autophagy could play a death-promoting role in Purkinje cells caused by asphyxial CA/CPR. Recent publications have confirmed that melatonin plays a role in the regulation of autophagy in ischemia/reperfusion injury (Feng et al., 2017; Zheng et al., 2014). In the present study, immunohistochemistry and western blot approaches showed that neuroprotective effect of melatonin was achieved by dramatic depletion of expressions of endogenous autophagic proteins (Beclin-1, Atg7 and LC3-II/LC3-I ratio). These results are supported by TEM images that showed that melatonin attenuated increased numbers of autophagic vacuoles, which correlate with our western blot results. Furthermore, PDOT treatment significantly concealed the protective effect of melatonin against autophagy-like process of Purkinje cell caused by asphyxial CA/CPR. Based on the results, we strongly suggest that melatonin plays an important role in preventing autophagy-like death of Purkinje cells caused by asphyxial CA/CPR via MT2.

The accumulation of ROS causes macromolecular damage, such as DNA oxidation and lipid peroxidation, leading to cellular damage and death (Allen and Bayraktutan, 2009). In the present study, melatonin treatment exhibited a significant decrease in the intensity and expression percentage of oxidized hydroethidine in the Purkinje cells induced by asphyxial CA/CPR. This result is consistent with previous studies reporting that melatonin is capable of modulating oxidative stress by reducing ROS in various ischemic studies (Chern et al., 2012; Ozacmak et al., 2009). In addition, exogenous treatment of melatonin induced the increased mRNA levels of SOD1, SOD2, CAT and GPx-1 in the cerebral and cerebellar cortex of aluminum-exposed rats (Esparza et al., 2005). Mayo et al. (2002) have reported that melatonin shows protection against cell death following 6-OHDA treatments and prevents a reduction in gene expressions of SOD1 and SOD2. In this study, SOD1 and SOD2 immunoreactivities in the Purkinje cells were significantly decreased from 12 h to 2 days after asphyxial CA/CPR. In the melatonin-CA group, however, their immunoreactivities did not decrease until 2 days after asphyxial CA/CPR. In addition, change patterns of SOD1 and SOD2 proteins were generally similar to their immunohistochemical changes. On the other hand, immunoreactivities of CAT and GPx were not detected in the Purkinje cells (data not shown), and their protein levels were not significantly changed following asphyxial CA/CPR. Previous study has suggested that the accumulation of ROS plays a vital role in the stimulation of autophagy under ischemia/reperfusion injury (Hariharan et al., 2011). In vitro studies also show that $O_2^{\bullet -}$ is involved in regulating autophagy, and this pathway is altered by SOD2 (Chen et al., 2009; Chen et al., 2007). Indeed, previous studies have shown that inhibitors of mitochondrial complex I and complex II induce autophagic cell death through increased $O_2^{\bullet -}$ production in transformed cell line HEK 293, and that overexpressing SOD2 blocks autophagy (Chen and Gibson, 2008; Chen et al., 2007). This is reversed by knocking down SOD2 via siRNA and potentiates cell death through increased $O_2^{\bullet -}$ production and induction of autophagy (Chen et al., 2007). This is supported by papers that show that the loss of SOD2 augments autophagy in the kidney following ischemia/reperfusion injury (Parajuli and MacMillan-Crow, 2013). Interestingly, we observed in this study that melatonin dramatically enhanced expressions of SODs in Purkinje cells caused by asphyxial CA/CPR, and this effect was cancelled by PDOT, indicating that the protective effect of melatonin might be due to the action of MT2 receptor.

In conclusion, this study is the first evaluation of Purkinje cell death via activation of autophagy using a rat model of asphyxial CA/CPR, showing that melatonin prevented autophagy-like death of Purkinje cells through a MT2 receptor. Furthermore, our present results demonstrated protective mechanisms of melatonin against autophagy-like death of Purkinje cells were achieved by dramatically reducing ROS, as well as, enhancing SOD1 and SOD2 protein expressions, which were dependent on MT2. Considering melatonin's high efficacy, these beneficial properties make melatonin suitable as a potential treatment against CA injury.

Declaration of Competing Interest

The authors declare that there are no conflicts of interest.

Acknowledgements

This work was supported by “Cooperative Research Program for Agriculture Science and Technology Development (Project No. PJ01329401)” Rural Development Administration, Republic of Korea, by Basic Science Research Program through the National Research Foundation of Korea (NRF) funded by the Ministry of Science, ICT & Future Planning (NRF-2017R1A2B4009079), by the Ministry of Education (NRF-2017R1D1A1B03031998), and by the Bio & Medical Technology Development Program of the NRF funded by the Korean government, MSIP (NRF-2015M3A9B6066835).

References

Allen, C.L., Bayraktutan, U., 2009. Oxidative stress and its role in the pathogenesis of ischaemic stroke. Int. J. Stroke 4, 461–470.
Brasko, J., Rai, P., Sabol, M.K., Patrikios, P., Ross, D.T., 1995. The AMPA antagonist NBQX provides partial protection of rat cerebellar Purkinje cells after cardiac arrest and resuscitation. Brain Res. 699, 133–138.
Cervantes, M., Morali, G., Letechipia-Vallejo, G., 2008. Melatonin and ischemia-reperfusion injury of the brain. J. Pineal Res. 45, 1–7.
Chen, Y., Gibson, S.B., 2008. Is mitochondrial generation of reactive oxygen species a trigger for autophagy? Autophagy 4, 246–248.
Chen, Y., McMillan-Ward, E., Kong, J., Israels, S.J., Gibson, S.B., 2007. Mitochondrial electron-transport-chain inhibitors of complexes I and II induce autophagic cell death mediated by reactive oxygen species. J. Cell Sci. 120, 4155–4166.
Chen, Y., Azad, M.B., Gibson, S.B., 2009. Superoxide is the major reactive oxygen species regulating autophagy. Cell Death Differ. 16, 1040–1052.
Chern, C.M., Liao, J.F., Wang, Y.H., Shen, Y.C., 2012. Melatonin ameliorates neural function by promoting endogenous neurogenesis through the MT2 melatonin receptor in ischemic-stroke mice. Free Radic. Biol. Med. 52, 1634–1647.
Drew, J.E., Barrett, P., Mercer, J.G., Moar, K.M., Canet, E., Delagrange, P., Morgan, P.J., 2001. Localization of the melatonin-related receptor in the rodent brain and peripheral tissues. J. Neuroendocrinol. 13, 453–458.
Eskelinen, E.L., 2005. Maturation of autophagic vacuoles in mammalian cells. Autophagy 1, 1–10.
Esparza, J.L., Gomez, M., Rosa Nogues, M., Paternain, J.L., Mallol, J., Domingo, J.L., 2005. Melatonin reduces oxidative stress and increases gene expression in the cerebral cortex and cerebellum of aluminum-exposed rats. J. Pineal Res. 39, 129–136.
Feng, D., Wang, B., Wang, L., Abraham, N., Tao, K., Huang, L., Shi, W., Dong, Y., Qu, Y., 2017. Pre-ischemia melatonin treatment alleviated acute neuronal injury after ischemic stroke by inhibiting endoplasmic reticulum stress-dependent autophagy via PERK and IRE1 signalings. J. Pineal Res. 62.
Fink, E.L., Alexander, H., Marco, C.D., Dixon, C.E., Kochanek, P.M., Jenkins, L.W., Lai, Y., Donovan, H.A., Hickey, R.W., Clark, R.S., 2004. Experimental model of pediatric asphyxial cardiopulmonary arrest in rats. Pediatr. Crit. Care Med. 5, 139–144.
Han, F., Boller, M., Guo, W., Merchant, R.M., Lampe, J.W., Smith, T.M., Becker, L.B., 2010. A rodent model of emergency cardiopulmonary bypass resuscitation with different temperatures after asphyxial cardiac arrest. Resuscitation 81, 93–99.
Hariharan, N., Zhai, P., Sadoshima, J., 2011. Oxidative stress stimulates autophagic flux during ischemia/reperfusion. Antioxid. Redox Signal. 14, 2179–2190.
Horn, M., Schlote, W., 1992. Delayed neuronal death and delayed neuronal recovery in the human brain following global ischemia. Acta Neuropathol. 85, 79–87.
Ichimura, Y., Kirisako, T., Takao, T., Satomi, Y., Shimonishi, Y., Ishihara, N., Mizushima, N., Tanida, I., Kominami, E., Ohsumi, M., Noda, T., Ohsumi, Y., 2000. A ubiquitin-like system mediates protein lipidation. Nature 408, 488–492.
Kihara, A., Kabeya, Y., Ohsumi, Y., Yoshimori, T., 2001. Beclin-phosphatidylinositol 3-kinase complex functions at the trans-Golgi network. EMBO Rep. 2, 330–335.
Kirino, T., 1982. Delayed neuronal death in the gerbil hippocampus following ischemia. Brain Res. 239, 57–69.
Koike, M., Shibata, M., Tadakoshi, M., Gotoh, K., Komatsu, M., Waguri, S., Kawahara, N., Kuida, K., Nagata, S., Kominami, E., Tanaka, K., Uchiyama, Y., 2008. Inhibition of autophagy prevents hippocampal pyramidal neuron death after hypoxic-ischemic injury. Am. J. Pathol. 172, 454–469.
Lee, C.H., Yoo, K.Y., Choi, J.H., Park, O.K., Hwang, I.K., Kwon, Y.G., Kim, Y.M., Won, M.H., 2010. Melatonin's protective action against ischemic neuronal damage is associated with up-regulation of the MT2 melatonin receptor. J. Neurosci. Res. 88, 2630–2640.

Lee, C.H., Park, J.H., Ahn, J.H., Won, M.H., 2016. Effects of melatonin on cognitive impairment and hippocampal neuronal damage in a rat model of chronic cerebral hypoperfusion. Exp. Ther. Med. 11, 2240–2246.
Lee, J.C., Park, J.H., Kim, I.H., Cho, G.S., Ahn, J.H., Tae, H.J., Choi, S.Y., Cho, J.H., Kim, D.W., Kwon, Y.G., Kang, I.J., Won, M.H., Kim, Y.M., 2017. Neuroprotection of ischemic preconditioning is mediated by thioredoxin 2 in the hippocampal CA1 region following a subsequent transient cerebral ischemia. Brain Pathol. 27, 276–291.
Liachenko, S., Tang, P., Hamilton, R.L., Xu, Y., 1998. A reproducible model of circulatory arrest and remote resuscitation in rats for NMR investigation. Stroke 29, 1229–1238 (discussion 1238-1229).
Liu, C., Gao, Y., Barrett, J., Hu, B., 2010. Autophagy and protein aggregation after brain ischemia. J. Neurochem. 115, 68–78.
Liu, L., Fang, Y.Q., Xue, Z.F., He, Y.P., Fang, R.M., Li, L., 2012. Beta-asarone attenuates ischemia-reperfusion-induced autophagy in rat brains via modulating JNK, p-JNK, Bcl-2 and Beclin 1. Eur. J. Pharmacol. 680, 34–40.
Mayo, J.C., Sainz, R.M., Antoli, I., Herrera, F., Martin, V., Rodriguez, C., 2002. Melatonin regulation of antioxidant enzyme gene expression. Cell. Mol. Life Sci. 59, 1706–1713.
Mizushima, N., Noda, T., Yoshimori, T., Tanaka, Y., Ishii, T., George, M.D., Klionsky, D.J., Ohsumi, M., Ohsumi, Y., 1998. A protein conjugation system essential for autophagy. Nature 395, 395–398.
Ozacmak, V.H., Barut, F., Ozacmak, H.S., 2009. Melatonin provides neuroprotection by reducing oxidative stress and HSP70 expression during chronic cerebral hypoperfusion in ovariectomized rats. J. Pineal Res. 47, 156–163.
Paine, M.G., Che, D., Li, L., Neumar, R.W., 2012. Cerebellar Purkinje cell neurodegeneration after cardiac arrest: effect of therapeutic hypothermia. Resuscitation 83, 1511–1516.
Pandi-Perumal, S.R., Srinivasan, V., Maestroni, G.J., Cardinali, D.P., Poeggeler, B., Hardeland, R., 2006. Melatonin: nature's most versatile biological signal? FEBS J. 273, 2813–2838.
Parajuli, N., MacMillan-Crow, L.A., 2013. Role of reduced manganese superoxide dismutase in ischemia-reperfusion injury: a possible trigger for autophagy and mitochondrial biogenesis? Am. J. Physiol. Ren. Physiol. 304, F257–F267.
Qu, X., Yu, J., Bhagat, G., Furuya, N., Hibshoosh, H., Troxel, A., Rosen, J., Eskelinen, E.L., Mizushima, N., Ohsumi, Y., Cattoretti, G., Levine, B., 2003. Promotion of tumorigenesis by heterozygous disruption of the beclin 1 autophagy gene. J. Clin. Invest. 112, 1809–1820.
Quillinan, N., Grewal, H., Deng, G., Shimizu, K., Yonchek, J.C., Strnad, F., Traystman, R.J., Herson, P.S., 2015. Region-specific role for GluN2B-containing NMDA receptors in injury to Purkinje cells and CA1 neurons following global cerebral ischemia. Neuroscience 284, 555–565.
Rami, A., Langhagen, A., Steiger, S., 2008. Focal cerebral ischemia induces upregulation of Beclin 1 and autophagy-like cell death. Neurobiol. Dis. 29, 132–141.
Sugawara, T., Lewen, A., Noshita, N., Gasche, Y., Chan, P.H., 2002. Effects of global ischemia duration on neuronal, astroglial, oligodendroglial, and microglial reactions in the vulnerable hippocampal CA1 subregion in rats. J. Neurotrauma 19, 85–98.
Tan, D.X., Manchester, L.C., Terron, M.P., Flores, L.J., Reiter, R.J., 2007. One molecule, many derivatives: a never-ending interaction of melatonin with reactive oxygen and nitrogen species? J. Pineal Res. 42, 28–42.
Thach, W.T., 1998. A role for the cerebellum in learning movement coordination. Neurobiol. Learn. Mem. 70, 177–188.
Tomas-Zapico, C., Coto-Montes, A., 2005. A proposed mechanism to explain the stimulatory effect of melatonin on antioxidative enzymes. J. Pineal Res. 39, 99–104.
Tsvetkov, A.S., Miller, J., Arrasate, M., Wong, J.S., Pleiss, M.A., Finkbeiner, S., 2010. A small-molecule scaffold induces autophagy in primary neurons and protects against toxicity in a Huntington disease model. Proc. Natl. Acad. Sci. U. S. A. 107, 16982–16987.
Wei, K., Wang, P., Miao, C.Y., 2012. A double-edged sword with therapeutic potential: an updated role of autophagy in ischemic cerebral injury. CNS Neurosci. Ther. 18, 879–886.
Welsh, J.P., Yuen, G., Placantonakis, D.G., Vu, T.Q., Haiss, F., O'Hearn, E., Molliver, M.E., Aicher, S.A., 2002. Why do Purkinje cells die so easily after global brain ischemia? Aldolase C, EAAT4, and the cerebellar contribution to posthypoxic myoclonus. Adv. Neurol. 89, 331–359.
Wen, Y.D., Sheng, R., Zhang, L.S., Han, R., Zhang, X., Zhang, X.D., Han, F., Fukunaga, K., Qin, Z.H., 2008. Neuronal injury in rat model of permanent focal cerebral ischemia is associated with activation of autophagic and lysosomal pathways. Autophagy 4, 762–769.
Yang, Z., Klionsky, D.J., 2010. Eaten alive: a history of macroautophagy. Nat. Cell Biol. 12, 814–822.
Yu, L., Sun, Y., Cheng, L., Jin, Z., Yang, Y., Zhai, M., Pei, H., Wang, X., Zhang, H., Meng, Q., Zhang, Y., Yu, S., Duan, W., 2014. Melatonin receptor-mediated protection against myocardial ischemia/reperfusion injury: role of SIRT1. J. Pineal Res. 57, 228–238.
Zheng, Y., Hou, J., Liu, J., Yao, M., Li, L., Zhang, B., Zhu, H., Wang, Z., 2014. Inhibition of autophagy contributes to melatonin-mediated neuroprotection against transient focal cerebral ischemia in rats. J. Pharmacol. Sci. 124, 354–364.